

## Polarization State of High-Order Harmonic Emission from Aligned Molecules

Jérôme Levesque,<sup>1,2</sup> Yann Mairesse,<sup>1</sup> Nirit Dudovich,<sup>1</sup> Henri Pépin,<sup>2</sup> Jean-Claude Kieffer,<sup>2</sup>  
P. B. Corkum,<sup>1</sup> and D. M. Villeneuve<sup>1,\*</sup>

<sup>1</sup>National Research Council Canada, Ottawa, Ontario, K1A 0R6, Canada

<sup>2</sup>INRS Énergie, Matériaux et Télécommunications, Varennes, Québec, J3X 1S2, Canada

(Received 17 May 2007; published 10 December 2007)

High harmonic emission in isotropic gases is polarized in the same direction as the incident laser polarization. Laser-induced molecular alignment allows us to break the symmetry of the gas medium. By using aligned molecules in high harmonic generation experiments, we show that the polarization of the extreme ultraviolet emission depends strongly on the molecular alignment and the orbital structure. Polarization measurements give insight into the molecular orbital symmetry. Furthermore, molecular alignment will allow us to produce attosecond pulses with time-dependent polarization.

DOI: [10.1103/PhysRevLett.99.243001](https://doi.org/10.1103/PhysRevLett.99.243001)

PACS numbers: 33.80.Rv, 42.50.Hz

In conventional nonlinear optics, the structure of the susceptibility tensor is dictated by the symmetry properties of the optical medium [1]. Nonlinear polarization spectroscopy has been applied in a wide range of experiments to determine the spatial symmetry of the nonlinear medium [2]. The background signal which originates, in most cases, from the nonexcited medium is a spatially symmetric process. Thus polarization techniques have become a major tool in nonlinear measurements, enhancing the signal-to-background ratio by many orders of magnitude [1]. In this Letter we extend polarization techniques into the highly nonlinear regime. We show how the polarization properties of the high harmonic generation process can resolve the spatial symmetry properties of molecular orbitals.

High harmonic emission is produced when gas phase atoms or molecules are ionized by an intense femtosecond laser pulse [3,4]. The relative phase and amplitude of high harmonics emitted from molecules are known to depend on the structure of the molecule and on its alignment [5–8]. This dependence has been linked to the structure and symmetry of the highest occupied molecular orbitals (HOMO) [8,9]. An image of a single molecular orbital has been obtained by recording high harmonic generation (HHG) spectra as a function of molecular alignment [10].

Until now, the probing of orbital structures by HHG has been limited to the measurement of the harmonics' spectral amplitudes. Both the quantum phase and the polarization of the imaged orbitals had to be determined by relying on assumptions of the molecular symmetry [10]. Such assumptions can only be made for the simplest molecules. This limitation can be overcome by measuring the polarization state of high harmonics. Polarimetry probes the off-diagonal components of the nonlinear tensor and thus provides an insight into the molecular orbital symmetry. This is possible because the polarization state contains information on the relative phase between the  $x$  and  $y$  components of the free-bound transition dipole moment. HHG polarimetry is a self-referencing measurement, be-

cause the quantum phase accumulated by the free electron is common to both polarization components and therefore does not influence the polarization state.

In this Letter we will show that high harmonics produced in aligned nitrogen, oxygen and carbon dioxide each show unique polarization features, due to their differing electronic structures. Until now, these features have been neither observed nor predicted. Just as polarization techniques became a basic building block in conventional nonlinear optics, their extension to HHG measurements is an important step towards imaging of complex molecules.

HHG polarization has previously been studied in atomic gases where the laser ellipticity was varied [11–13]. In that case, the HHG polarization state was affected by the angle of the recollision electron rather than by the electronic structure. The approach we adopt here is different, as we modify the gas medium while keeping the laser polarization linear. The molecular medium is controlled by laser-induced molecular alignment. In this technique a strong laser pulse creates a rotational wave packet that periodically rephases and leads to an alignment of the molecular axis in a direction parallel to the laser polarization. This approach is described in greater detail elsewhere [14–16] and has been used in previous HHG experiments [8,10,17,18].

In Fig. 1 we show the experimental setup. An interferometer splits the initial laser pulse in two: (1) an alignment pulse (to align molecules) and (2) an ionizing pulse (to generate high harmonics). Both pulses were verified to be linearly polarized. The alignment pulse's polarization could be rotated by an angle  $\theta$  with respect to the ionizing pulse by a motorized half-wave plate [HWP1 in Fig. 1(a)]. The polarization of the two pulses could also be rotated together, by an angle  $\phi$ , using another motorized half-wave plate (HWP2). Thus the polarization direction of both pulses could be independently controlled.

Both laser pulses were focused into a pulsed supersonic gas jet containing the sample gas. The 3 atm backing pressure gave a rotational temperature of  $\sim 20$  K. The first laser pulse creates a rotational wave packet. The second

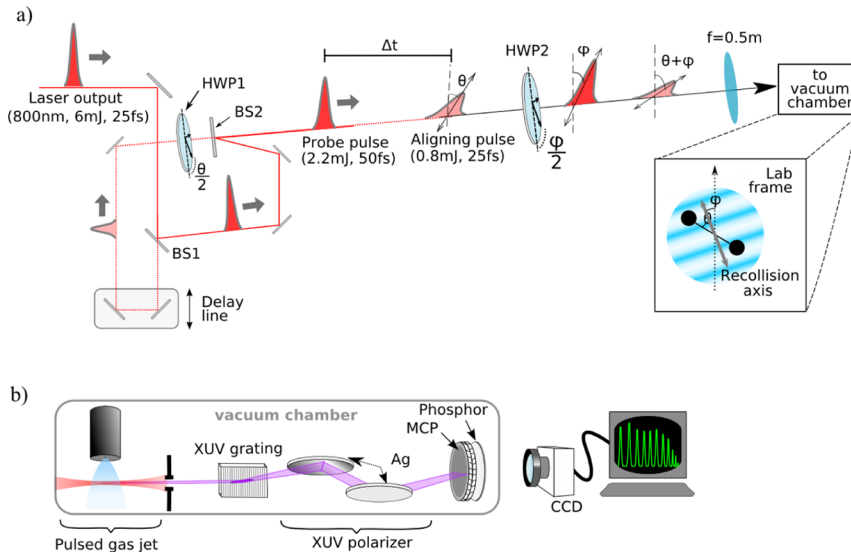


FIG. 1 (color online). Diagram of the experimental setup. (a) The Ti:sapphire laser pulse is split into two pulses whose polarization can be controlled independently. The first pulse aligns the molecular sample, and the second delayed pulse produces high harmonics during a fractional revival of the rotational wave packet. (b) The XUV emission is recorded with a spectrometer that includes two silver mirrors that serve as polarizers.

laser pulse was delayed in the order of tens of picoseconds after the first pulse, timed to coincide with a rotational revival of each molecular species. This laser pulse was more intense than the first, enough to ionize the aligned molecules and produce high harmonic emission. The harmonic emission was recorded by an extreme ultraviolet (XUV) spectrometer and an MCP detector [Fig. 1(b)]. A pair of silver mirrors at  $20^\circ$  and  $25^\circ$ , respectively, was placed between the XUV grating and the detector to act as a polarizer [13].

In general, the polarization state of an electromagnetic field cannot be determined simply by recording two orthogonal amplitudes. The transmission through a linear polarizer must be recorded over a  $180^\circ$  rotation of the polarizer. In an optical polarimeter, the analyzing polarizer is rotated. In the present case it was impractical to rotate the entire spectrometer, and so the polarization vectors of both laser pulses were simultaneously rotated by HWP2. Because the polarimeter's contrast was not perfect, it was calibrated at each harmonic order using atomic argon in place of a molecule. From symmetry considerations, HHG from argon will be linearly polarized parallel to the fundamental beam polarization. The HHG signal follows a  $\cos^2$  function characteristic of Malus' law.

In Fig. 2 we show the polarization rotation measurements for harmonics generated in aligned  $N_2$ ,  $O_2$ , and  $CO_2$ , both as lines and as colors. The laser polarization is vertical in this graph, and zero orientation means the molecular axis is vertical. For each molecule, we scanned the molecular alignment from  $-90^\circ$  to  $+90^\circ$  and observed the rotation of the high harmonics polarization. In general, the harmonic emission can be elliptically polarized, depending on the symmetry of the molecular orbitals. However, the measured harmonics were found to be linearly polarized to within experimental error for all three molecules measured.

The polarization rotation in 2D can be represented by a single parameter  $\rho = \arctan(E_x/E_y)$  where  $E_x$ ,  $E_y$  are the

XUV fields in the  $\hat{x}$ ,  $\hat{y}$  directions (laser is polarized along  $\hat{y}$ ). In Fig. 3 measurements of  $\rho$  are shown for particular alignment angles. For  $N_2$  aligned at  $\pm 45^\circ$  we observe that below H23, the polarization is rotated in the same direction as the molecular axis, while for harmonics above H23 it is rotated in the opposite direction.

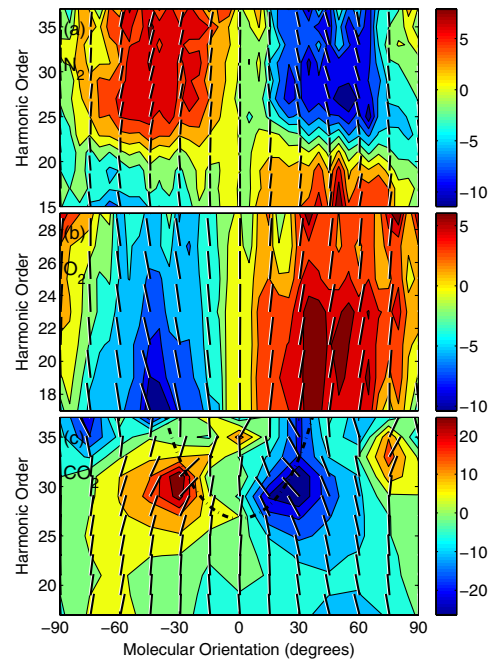


FIG. 2 (color online). Direction fields representing the polarization of harmonics produced in aligned (a)  $N_2$ , (b)  $O_2$ , and (c)  $CO_2$ . The lines represent the measured values of the polarization direction. The driving laser is vertically polarized. For an atom, all lines would be vertical. The color represents the rotation angle from vertical in degrees. For positive molecular orientation, a clockwise rotation of the line means that the polarization direction is following the molecular axis. The same information is presented as both lines and as color contours.

The O<sub>2</sub> molecule shows different features. For  $\pm 45^\circ$  alignments, the polarization is rotated in the same direction as the molecule for all harmonic orders. In CO<sub>2</sub> the behavior is opposite—the polarization is counterrotated with respect to the molecule. This feature is strongest at  $\pm 30^\circ$ .

We present a theoretical analysis of high harmonic emission in aligned molecules, based on the strong-field approximation. We take  $y$  as the laser polarization axis. The momentum of the free electron,  $k$ , is also along  $y$ . The molecule lies in the  $xy$  plane. Since the recollision electron is the same for both polarizations, we can ignore the recollision amplitude and phase, and concentrate on the dipole contribution.

We approximate the continuum electron by a set of plane waves,  $\psi_k = e^{iky}$  for each electron wave number  $k$  which is in turn determined by the observed harmonic frequency  $\Omega$  by  $\Omega = k^2/2 + I_p$  and  $I_p$  is the ionization potential of the molecule. The transition dipole is given by [10]

$$\vec{d}(k; \theta) = \langle \psi_0(\vec{r}; \theta) | \vec{r} | e^{iky} \rangle. \quad (1)$$

Here the notation  $\psi_0(\vec{r}; \theta)$  refers to the ground state wave function rotated by an angle  $\theta$  from the  $y$  axis in the laboratory frame. Angle  $\theta$  corresponds to the horizontal axis labeled “Molecular Orientation” in Fig. 2 and the angles in Fig. 3. (We also include additional terms, not shown, due to multielectron effects upon recombination [19,20]). The transition dipole is a vector quantity with components  $d_x$  and  $d_y$ . The direction defined by this dipole corresponds to the direction of the polarization axis that we measure experimentally.

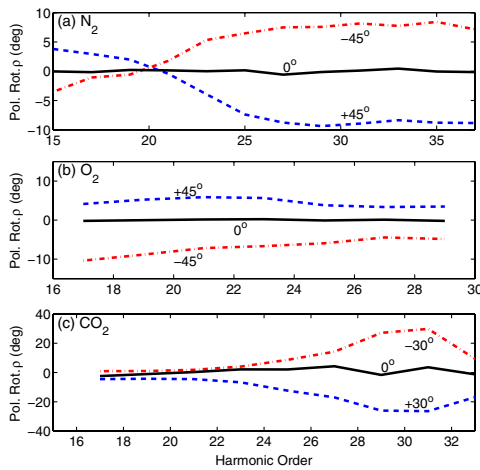


FIG. 3 (color online). Measured values of  $\rho(\omega)$ , the rotation of the polarization axis from the driving laser’s polarization axis, for harmonics generated in (a) N<sub>2</sub> aligned at  $0^\circ$  and  $\pm 45^\circ$ , (b) O<sub>2</sub> aligned at  $0^\circ$  and  $\pm 45^\circ$ , and (c) CO<sub>2</sub> aligned at  $0^\circ$  and  $\pm 30^\circ$ . Here  $\rho$  represents the angle between the laser polarization axis and the polarization of the emitted XUV harmonics. Positive  $\rho$  means that the XUV polarization has rotated in the direction of the molecular axis. These cuts are taken from the data presented in Fig. 2.

This model predicts that the XUV should be linearly polarized for all the molecules used, as was observed. Any orbital with inversion symmetry will have the same phase for both components, because each axis has the same symmetry.

The calculated  $\rho = \arctan(d_x/d_y)$ , using the  $3\sigma_g$  HOMO of N<sub>2</sub> calculated by GAMESS [21], is shown in Fig. 4. The theoretical calculation shows qualitative agreement with the experiment in Fig. 2(a), as will be discussed below. The HHG spectral amplitude from N<sub>2</sub> displays a minimum in the spectrum at H25, independent of molecular angle; this can be seen in the normalized experimental data of Itatani *et al.* [10]. In the present experiment, we see a change in sign of the polarization rotation at H21, independent of angle.

Both of these observations are consistent with a component of the transition dipole  $\vec{d}$  going through zero. In Fig. 4, at  $30^\circ$ , the polarization direction goes from 1 o’clock at H15 to 5 o’clock at H41. This means that  $d_y$ , the parallel component, changes sign around H27, but  $d_x$ , the perpendicular component, does not change sign. This is consistent with the experimental results in Fig. 2(a), if we assume that we cannot resolve  $d_y$  going through zero. We do not expect good agreement at the resonant frequency, where one or both polarization components go through zero. Unlike the model, in the experiment we cannot measure the sense of the polarization, so there are no arrow heads in Fig. 2. The apparent rotation of the polarization from 1 o’clock at H15 to 11 o’clock at H37 is in fact consistent with the model since we cannot distinguish experimentally between 11 o’clock and 5 o’clock.

The theoretical model has to be generalized for CO<sub>2</sub>, since the plane wave approximation breaks down at  $0^\circ$  and  $90^\circ$  due to the nodal plane of the  $\pi_g$  HOMO. Nevertheless, we can associate the regions of strong polarization rotation in CO<sub>2</sub> with a sign change in both  $d_x$  and  $d_y$ . As in N<sub>2</sub>, this sign change correlates with an observed minimum in the HHG emission of CO<sub>2</sub>. The HOMO of CO<sub>2</sub> has two localized components centered over each O<sub>2</sub> atom. This allows us to determine the position of the zeros in the emission using the so-called “two-center model” [8,9,17]. The dotted line in Fig. 2(c) shows the location of the observed minimum based on the two-center model and can be seen to coincide with the region of maximum polarization rotation.

Why is it that, if the polarization rotation in N<sub>2</sub> and CO<sub>2</sub> is caused by a zero crossing of a component of the transition dipole  $\vec{d}$ , they manifest different behavior? It is due to the differing symmetries of the HOMOs. In N<sub>2</sub>, only the parallel component goes through zero while the perpendicular component remains nonzero. In CO<sub>2</sub>, both the parallel and perpendicular components go through zero at about the same point. The actual region where this occurs is difficult to resolve experimentally because as the magnitude of the harmonic signal decreases, the experimental error of our measurement increases.

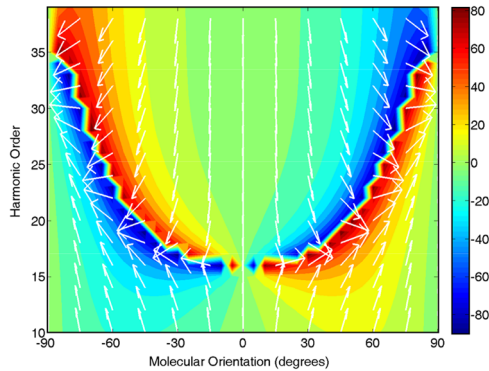


FIG. 4 (color online). Predictions of the simple model for the polarization direction of high harmonic emission from  $N_2$ . It shows qualitative agreement with the measurements for angles less than  $60^\circ$ . Note that the experimental measurements of polarization only measure the angle from the vertical, and so there are no arrowheads in Fig. 2. Conversely, the model predicts an actual direction for the transition dipole, which can be seen to flip at certain harmonics. As in Fig. 2, the same information is presented as both vectors and as colors.

Thus the polarization measurement distinguishes between the  $\sigma_g$  and  $\pi_g$  symmetries of the two molecules.

Molecular alignment offers a handle to control the polarization state of high harmonic emission on an attosecond time scale. The basic physics of attosecond pulse generation requires that each pulse in the train of attosecond pulses is chirped. The polarization that we measure in the harmonics tells us about the polarization within an individual attosecond pulse in the pulse train. Our measurements require that the attosecond pulses produced from aligned molecules have time-dependent polarization. We control the polarization dynamics by controlling the molecule.

We can use aligned molecules to generate elliptically polarized attosecond xuv radiation. When harmonics are generated in  $N_2$  aligned at  $45^\circ$  or  $CO_2$  aligned at  $30^\circ$ , a harmonic component perpendicular to the laser polarization is produced. If these molecules are mixed with an atomic gas, for example, the perpendicular component of the harmonic polarization would come only from the molecule while the parallel component would come from the superposition of the atomic and molecular contributions. The atom can emit radiation at a different phase than the molecule due to differing orbital symmetry or a change in the projected size of the molecule as we rotate it. In this case, phase retardation is induced between the parallel and perpendicular components of the polarization, leading to elliptical polarization of the XUV radiation. This approach also offers a way to measure the relative phase between different molecules.

Polarization based measurements can be applied to subtract the background in many experiments. For example, the harmonic signal from randomly aligned molecules is

polarized along the laser polarization; therefore, a time resolved measurement of the perpendicular component will have a zero background. Combining the high sensitivity to the molecular structure with the background subtraction, polarization techniques becomes a powerful tool in imaging the temporal evolution of a molecular orbital during a chemical reaction.

We acknowledge the Natural Sciences and Engineering Council of Canada for financial support.

\*david.villeneuve@nrc.ca

- [1] R.W. Boyd, *Nonlinear Optics* (Academic Press, San Diego, CA, 2003), 2nd ed.
- [2] N. Bloembergen, *Nonlinear Optics* (Benjamin, New-York, 1964).
- [3] A. L'Huillier and P. Balcou, *Phys. Rev. Lett.* **70**, 774 (1993).
- [4] M. Lewenstein, P. Balcou, M. Y. Ivanov, A. L'Huillier, and P. B. Corkum, *Phys. Rev. A* **49**, 2117 (1994).
- [5] Y. Liang, A. Augst, S.L. Chin, Y. Beaudoin, and M. Chaker, *J. Phys. B* **27**, 5119 (1994).
- [6] N. Hay, R. Velotta, M. Lein, R. de Nalda, E. Heesel, M. Castillejo, and J. Marangos, *Phys. Rev. A* **65**, 053805 (2002).
- [7] M. Lein, N. Hay, R. Velotta, J. Marangos, and P. Knight, *Phys. Rev. A* **66**, 023805 (2002).
- [8] J. Itatani, D. Zeidler, J. Levesque, M. Spanner, D.M. Villeneuve, and P.B. Corkum, *Phys. Rev. Lett.* **94**, 123902 (2005).
- [9] T. Kanai, S. Minemoto, and H. Sakai, *Nature (London)* **435**, 470 (2005).
- [10] J. Itatani, J. Levesque, D. Zeidler, H. Niikura, H. Pépin, J.-C. Kieffer, P. B. Corkum, and D. M. Villeneuve, *Nature (London)* **432**, 867 (2004).
- [11] F. A. Weihe, S. K. Dutta, G. Korn, D. Du, P. H. Bucksbaum, and P. L. Shkolnikov, *Phys. Rev. A* **51**, R3433 (1995).
- [12] F. A. Weihe and P. H. Bucksbaum, *J. Opt. Soc. Am. B* **13**, 157 (1996).
- [13] P. Antoine, B. Carré, A. L'Huillier, and M. Lewenstein, *Phys. Rev. A* **55**, 1314 (1997).
- [14] F. Rosca-Pruna and M. J. J. Vrakking, *Phys. Rev. Lett.* **87**, 153902 (2001).
- [15] H. Stapelfeldt and T. Seideman, *Rev. Mod. Phys.* **75**, 543 (2003).
- [16] P. W. Dooley, I. Litvinyuk, K. F. Lee, D. M. Rayner, M. Spanner, D. M. Villeneuve, and P. B. Corkum, *Phys. Rev. A* **68**, 023406 (2003).
- [17] C. Vozzi, F. Calegari, E. Benedetti, J.-P. Caumes, G. Sansone, S. Stagira, M. Nisoli, R. Torres, E. Heesel, and N. Kajumba *et al.*, *Phys. Rev. Lett.* **95**, 153902 (2005).
- [18] K. Miyazaki, M. Kaku, G. Miyaji, A. Abdurrouf, and F. H. M. Faisal, *Phys. Rev. Lett.* **95**, 243903 (2005).
- [19] S. Patchkovskii, Z. Zhao, T. Brabec, and D. M. Villeneuve, *Phys. Rev. Lett.* **97**, 123003 (2006).
- [20] S. Patchkovskii, Z. Zhao, T. Brabec, and D. M. Villeneuve, *J. Chem. Phys.* **126**, 114306 (2007).
- [21] M. W. Schmidt *et al.*, *J. Comput. Chem.* **14**, 1347 (1993).